The k_1 value for phenylacetylene toward each thiyl radical is smaller than the corresponding value for styrene by a factor of ca. 25, whereas it is larger than that for 1-pentyne by a factor of ca. 70. If PhSCH=ĊPh is the linear π radical,[5,6,22] the reactivity ratio of phenylacetylene to styrene must be attributed to the different conjugation properties of the π radicals, which involve the sp- and sp^2-hybridized carbons, respectively. However, the spin densities of the phenyl ring of the α-styryl radical calculated on the assumption of the linear π radical were practically the same as those of the benzyl radical;[23,26] thus, such difference in the conjugation properties between both π radicals is not so large. The high reactivity of PhSCH=ĊPh toward oxygen or hydrogen donors, as deduced from Figure 1, was not observed in the case of styrene or methyl acrylate (Figure 2); this seems to correspond to an increase in the s character of the half-filled orbital of PhSCH=ĊPh. If PhSCH=ĊPh is the σ radical, we must consider the stabilization of an unpaired electron in the sp^2 orbital by the interaction with the adjacent phenyl ring through space[27] or through σ bonds; however, there may be a doubt whether such interaction is strong enough to explain the high reactivity of phenylacetylene compared to 1-pentyne (ca. 70 times). From our data for the reactivities, another possible explanation, that the actual α-styryl-type radical has an intermediate character between the localized σ radical and the linear π radical, was suggested.

In summary, we have estimated the absolute rate constants for the addition reactions of p-$XC_6H_4S\cdot$ to CH≡CR and CH_2=CHR (R = Ph, alkyl, and $COOCH_3$) by flash photolysis. From the Hammett plots, it was suggested that the reactivities are mainly determined by the stabilities of the adduct radicals. An unpaired electron of $PhSCH_2\dot{C}HCOOCH_3$ is stabilized with the interaction with the ester group, whereas PhSCH=ĊCOOCH$_3$ may be a localized σ radical. PhSCH=ĊPh may have an intermediate character between the σ radical and the π radical.

(25) There is a possibility that the prediction of the σ and π radicals from the MO energies is reversed by the methods used for the MO calculations: Kasai, P. H.; Clark, P. A.; Whipple, E. B. *J. Am. Chem. Soc.* **1970**, *92*, 2640.
(26) Lloyd, R. V.; Wood, D. E. *Mol. Phys.* **1971**, *20*, 735.
(27) Intramolecular charge-transfer interaction between the electron-deficient σ orbital and the electron-rich phenyl ring can be considered as a through-space interaction. In the case of PhSCH=ĊCOOCH$_3$, such interaction cannot be expected since both the carbonyl double bond and the σ orbital are electron deficient.

Experimental Section

Commercially available phenylacetylene, 1-pentyne, methyl propiolate, 1-hexene, and methyl acrylate were distilled under reduced pressure before use. Diphenyl disulfides were purified by recrystallization from ethanol. Solvents were of spectrophotometric grade. The oxygen concentration in solution was controlled by dissolving oxygen under an appropriate pressure after degassing up to 10^{-5} torr; the oxygen concentration was calculated from Henry's law by using the reported oxygen concentration in aerated benzene (1.9×10^{-3} M).[14] The flash photolysis experiments were made at room temperature controlled at 23 ± 1 °C. A xenon flash photolysis apparatus of standard design was used; the flash energy was ca. 100 J, and the half-duration of the xenon flash lamps was ca. 10 μs.

Registry No. p-$BrC_6H_4S\cdot$, 31053-90-4; p-$ClC_6H_4S\cdot$, 31053-91-5; $C_6H_5S\cdot$, 4985-62-0; p-$CH_3C_6H_4S\cdot$, 31053-92-6; p-(t-C_4H_9)$C_6H_4S\cdot$, 81372-23-8; p-$CH_3OC_6H_4S\cdot$, 31053-93-7; CH_2=$CHCOOCH_3$, 96-33-3; CH_2=CHC_4H_9, 592-41-6; CH≡CPh, 536-74-3; CH≡CC_3H_7, 627-19-0; CH≡$CCOOCH_3$, 922-67-8.

Determination of the Orientation of Aromatic Molecules Adsorbed on Platinum Electrodes.[1,2] The Effect of Solute Concentration

Manuel P. Soriaga and Arthur T. Hubbard*

Contribution from the Department of Chemistry, University of California, Santa Barbara, California 93106. *Received December 14, 1981*

Abstract: Accurate measurements of the amounts of aromatic molecules adsorbed on smooth polycrystalline platinum electrodes in aqueous solutions are reported as a function of concentration. The measurements were made by electrochemical methods using thin-layer cells. A plot of adsorbed amount against concentration shows that most of the subject compounds display multiple plateaus separated by abrupt transitions to higher densities at higher concentrations. Comparison of plateau values with model calculations, based upon covalent and van der Waals radii tabulated by Pauling, reveals that a series of definite orientations are adopted as the adsorbate concentration is increased; each individual orientation was stable over an appreciable range of concentration. Twenty-six compounds, representing a variety of structures and chemical properties, were studied: simple diphenols; alkyldiphenols; polyhydroxybenzenes; halogenated diphenols; N heteroaromatics; diphenols having surface-active side chains; polycyclic phenols and quinones; and hydroquinone mercaptans.

The orientation of aromatic molecules adsorbed from solution on smooth polycrystalline platinum electrodes has been studied as a function of adsorbate molecular structure and supporting electrolyte.[1,2] At low concentrations (≤0.1 mM), in the absence of competing surfactants, aromatic molecules generally adopt a flat orientation on the Pt surface. Deviations from this orientation occur for heteroaromatics and when electronegative or surface-active functional groups are present on the aromatic ring.[1] Also, when a layer of molecules adsorbed in the flat orientation was exposed to a solution of a surface-active anion, iodide, reorientation to an edgewise orientation occurred for most of the compounds.[2] The present article describes the concentration dependence of the orientations of 26 aromatic compounds adsorbed on platinum.

(1) Soriaga, M. P.; Hubbard, A. T. *J. Am. Chem. Soc.* **1982**, *104*, 2735.
(2) Soriaga, M. P.; Hubbard, A. T. *J. Am. Chem. Soc.* **1982**, *104*, 2742.

Measurement of Adsorbed Aromatics

An accurate method, based upon thin-layer electrochemistry, for measurement of the amount of aromatic compound adsorbed on Pt has been described.[1] Only details unique to the present study

0002-7863/82/1504-3937$01.25/0

will be included here. When working with very dilute solutions of strongly adsorbing compounds in small-volume thin-layer cells, it was necessary to fill the thin-layer cavity with surfactant repeatedly in order to satisfy the adsorptive demands of the surface. If during the first filling *all* of the solute was taken up by the electrode surface, solute peaks were absent from subsequent voltammetric scans. In that case the amount of material taken up during the first filling was found from eq 1, where Γ_1 (mol/cm^2)

$$\Gamma_1 = VC^0/A \quad (1)$$

was the interfacial concentration, C^0 the initial solute concentration, V the thin-layer cell volume, and A the electrode surface area. If a number of fillings, k, were required in order to build up the adsorbed layer, then the total adsorbed amount present at that stage was

$$\Gamma_1 + \Gamma_2 + \ldots + \Gamma_k = kVC^0/A \quad (2)$$

The next filling ($k + 1$) led to a dissolved excess of surfactant, detected by thin-layer voltammetry[1] and quantitated by thin-layer coulometry; the adsorbed amount was found from the dissolved excess by the Faraday law:

$$\Gamma_{k+1} = \frac{Q_{k+2} - Q_{k+1}}{nFA} \quad (3)$$

The final ($k + 2$) filling led to no further adsorption and was used to determine the bulk solute concentration, C^0

$$C^0 = (Q_{k+2} - Q_b)/nFV \quad (4)$$

where Q_b was the electrolytic charge due to background reactions occurring under conditions identical to $k + 2$, except that dissolved surfactant had been rinsed from the thin-layer cavity with pure electrolyte. The final interfacial concentration was the sum of the $k + 1$ components Γ_j defined by eq 1–3.

$$\Gamma = \sum_{j=1}^{k+1} \Gamma_j \quad (5)$$

A few of the adsorbed compounds displayed reversible electrochemical reactivity at the same potentials where unadsorbed species reacted. The amount of this adsorbed electroactive material was determined, as a function of concentration, as follows.[3] The clean electrode was exposed to surfactant solution of a given concentration and then was rinsed with pure supporting electrolyte to remove excess dissolved surfactant; reversibly electroactive material adhering to the electrode was then detected by thin-layer voltammetry and determined by thin-layer coulometry.

Experimental Section

Preparation of electrodes, electrolytes, and a majority of the surfactants was described previously.[1] Adsorbed amounts were determined at concentations from 2.5 μM to 5 mM. In most cases, the upper concentration limit was imposed by the solubility of the aromatic compound in aqueous 1 M perchlorate, while the lower limit depended on the volume and area of the thin-layer cell (typically 4.08 μL and 1.18 cm^2). For measurements below 25 μM, a cell having a larger volume (27.7 μL) but similar area (0.979 cm^2) was used, in order to minimize the number of fillings required for saturation of the surface. Electrolytic charge Q was determined by means of an operational-amplifier circuit and a four-place digital voltmeter.

Compound **20**, 2,5-dihydroxy-4-methylbenzyl mercaptan was generously provided by D. L. Fields[4] of Eastman Kodak Co. Compound **22**, 2,2′,5,5′-tetrahydroxybiphenyl, was prepared by Professor Clifford S. Benton of Westmont College using published procedures.[5] Compound **18**, 3-hydroxytyramine (dopamine), was purchased from Sigma Chemical Co. (St. Louis, MO) as the hydrochloride salt. Addition of 11 M $HClO_4$ to an aqueous solution of dopamine hydrochloride, with cooling in an ice bath, precipitated the perchlorate salt which was filtered under nitrogen and dried in vacuo.

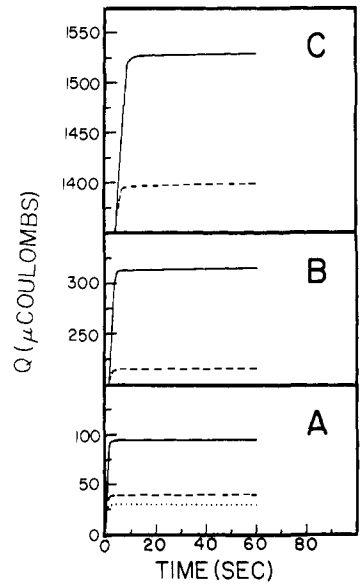

Figure 1. Thin-layer coulometric curves for the reduction of unadsorbed benzoquinone to hydroquinone at (A) 0.096 mM, (B) 0.35 mM, and (C) 1.9 mM solute concentration in 1 M $HClO_4$ supporting electrolyte: (---) one rinse, Q_1; (—) two rinses, Q_2; (···) background, Q_b. Potential step was from 0.56–0.20 V vs. the AgCl (1 M Cl$^-$) reference electrode (thin-layer volume, V, ≈ 4.08 μL; platinum electrode area, A, = 1.18 cm^2; temperature = 296 ± 1 K).

Results

Figure 1 shows typical thin-layer coulometric curves for the reduction of benzoquinone to hydroquinone for one (Q_1, dashed curve) and two (Q_2, solid curve) fillings at specified concentrations; for comparison, the background electrolytic charge, Q_b (dotted curve), is also shown. The difference between Q_2 and Q_1 for 0.096 mM hydroquinone (Figure 1A), although readily measured, amounts to a relatively low packing density. $Q_2 - Q_1$ is almost twice as large at 1.9 mM (Figure 1C), indicating an almost twofold increase in the amount of adsorbed material. Coulometric curves such as those shown in Figure 1 were obtained for each of the 26 subject compounds, several trials at each concentration. A detailed tabulation of results appears in Table I. Adsorbed amounts are expressed as interfacial concentration, Γ (mol cm^{-2}), as well as the average area (Å^2) occupied by an adsorbed molecule, σ. The values of Γ are graphed vs. concentration, expressed as the negative logarithm, in Figure 2. Most of the compounds display multiple plateaus separated by abrupt transitions to higher Γ at higher concentrations, which could be due to (i) adsorption into voids remaining in the layer after exposure to lower concentrations, (ii) changes in orientation from inefficiently packed ones to others affording denser packing, and/or (iii) multilayer condensation. The first possibility is realized only for compound **11**, tetrafluorohydroquinone, which is adsorbed only weakly and therefore has not yet reached limiting coverage at the lower concentrations.[1,2] As in gas–solid systems, multilayer adsorption of organics from solution onto nonporous adsorbents is reversible and shows an asymptotic increase in coverage at concentrations approaching the solubility of the adsorbate in the solution phase.[6] In contrast to this, the present data show that an increase in coverage beyond that for the first plateau is not observed for some compounds; others increase and then level off, rather than increasing indefinitely as for multilayers. As shown below, the present transitions to higher packing density are irreversible, unlike those for multilayer formation. Therefore, molecular reorientation within the adsorbed monolayer remains the most plausible explanation for the concentration-induced changes in Γ.

Transitions in Γ starting from the flat orientation at low coverage occur at roughly the same concentration, about 0.13 mM,

(3) Soriaga, M. P.; Wilson, P. H.; Hubbard, A. T.; Benton, C. S. *J. Electroanal. Chem.*, in press.
(4) Fields, D. L.; Miller, J. B.; Reynolds, D. D. *J. Org. Chem.* **1965**, *30*, 3962.
(5) Ullmann, F. *Justus Liebigs Ann. Chem.* **1904**, *332*, 68.
(6) Adamson, A. W. "The Physical Chemistry of Surfaces"; Wiley: New York, 1976.

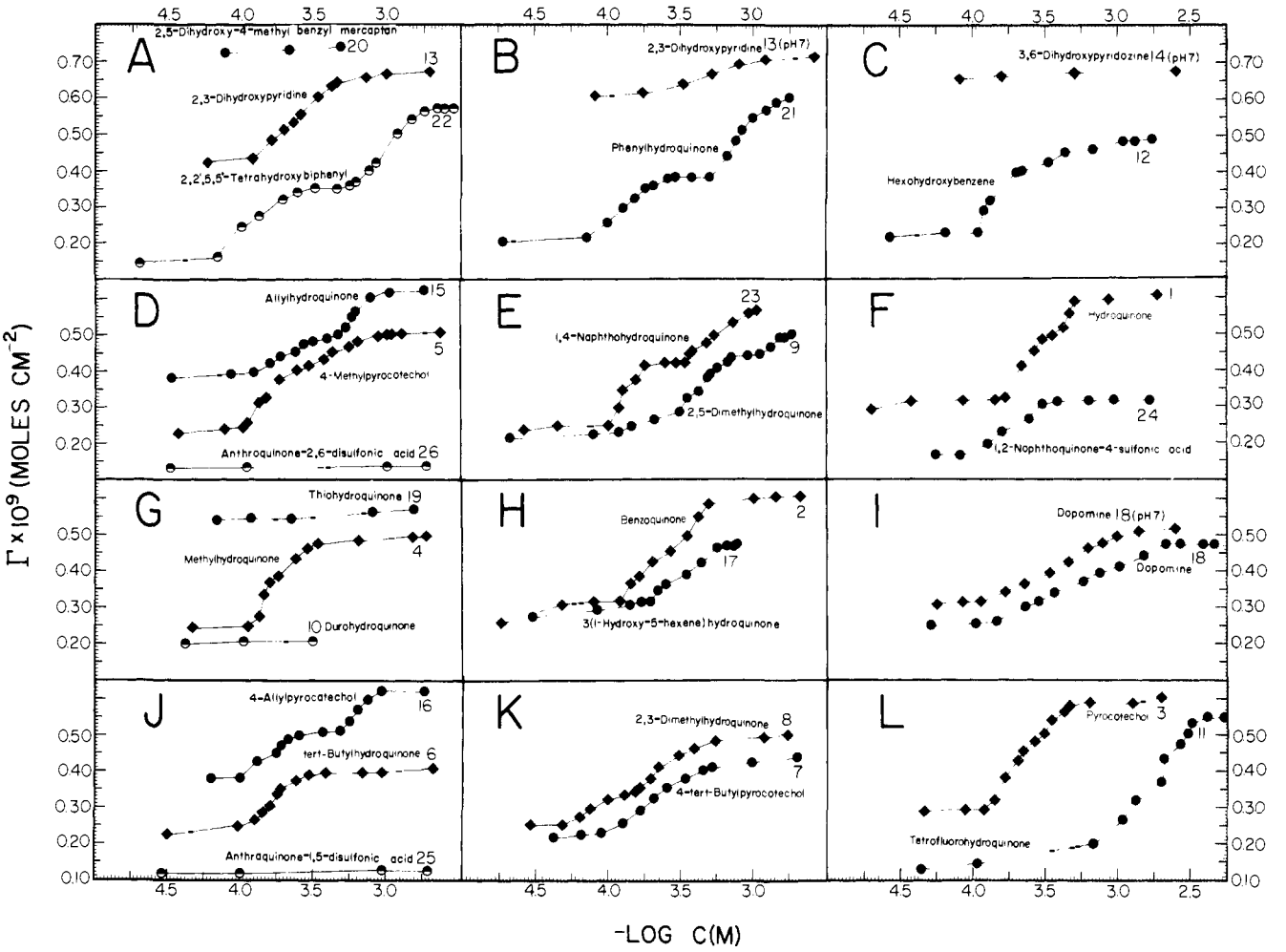

Figure 2. Adsorption data, expressed as Γ (mol cm^{-2}), as a function of solute concentration. The sizes of the points represent the average experimental deviation, and the numbers on the graph identify compounds as listed in Table I. The solid lines interconnect the experimental points and do not represent any theoretical curve. A detailed listing of data appears in Table I.

for all compounds except **8** and **9**. This suggests that the adsorption parameters of these compounds are qualitatively similar, at least for the first orientational transition.[3]

The coverages, σ_p, at the point of minimal slope on each plateau of Figure 2, are also indicated in Table I. Comparison of σ_p with theoretical σ values, tabulated in a previous article,[1] indicates the probable orientations of the adsorbed aromatics at each plateau. Each observed σ_p is found to coincide with a σ value calculated for a specific orientation, except, as expected, for compounds having multiple surface-active functional groups [**13** and **15–18** (pH 7)] for which a mixture of two or more orientations is indicated.

In addition to measurement of the amount of surfactant adsorbed on *clean* Pt, experiments were performed in which the Pt electrode was *precoated* with hydroquinone or pyrocatechol, rinsed in pure supporting electrolyte, and reexposed to one of these surfactants at the concentration specified. The results, Table II, lead to the following generalizations: (i) the adsorption of aromatic, whether in the flat or edgewise orientation, is *irreversible*; (ii) the orientational transition from the low-coverage (flat) to the high-coverage form is *irreversible*; and (iii) dissimilar aromatic compounds may induce transitions of one another. The irreversibility of the adsorption transitions provides further evidence that the increase in coverage with concentration is due to changes within an adsorbed monolayer rather than to multilayer condensation.

Figure 3 shows thin-layer current–potential curves of the dissolved (unadsorbed) and adsorbed forms of 2,2′,5,5′-tetrahydroxybiphenyl, **22**, and 2,5-dihydroxy-4-methylbenzyl mercaptan, **20**, in 1 M $HClO_4$ supporting electrolyte. The formal potentials of the dissolved and adsorbed forms of compound **20**,

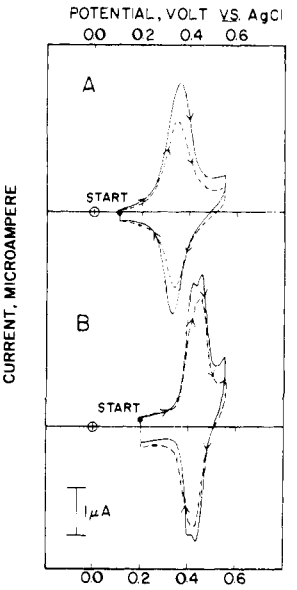

Figure 3. Thin-layer current–potential curves for unadsorbed (—) and adsorbed (- - -) species: (A) 2,5-dihydroxy-4-methylbenzyl mercaptan and (B) 2,2′,5,5′-tetrahydroxybiphenyl. The concentration of the dissolved reactant was 0.1 mM, and the sweep rate, r, was 2 mV s^{-1}. All other experimental conditions were as in Figure 1.

Figure 3A, are essentially identical (0.35 V against AgCl reference electrode). In contrast, the adsorbed form of **22**, Figure 3B, shows only one peak at 0.44 V while the dissolved form shows two peaks

Table I. Adsorption Data: Aromatic Compounds Adsorbed on Pt from Solution at Various Concentrations[a]

C, mM	Γ,[b] nmol/cm^{-2}	σ, Å^2/molecule
	Hydroquinone (1)	
0.020	0.294	56.5
0.037	0.313	53.1
0.086	*0.315*	*52.7*[c]
0.140	0.355	46.8
0.165	0.381	43.6
0.214	0.411	40.4
0.261	0.454	36.6
0.300	0.484	34.3
0.350	0.498	33.3
0.420	0.519	32.0
0.460	0.555	29.9
0.500	0.590	28.1
0.880	*0.595*	*27.9*[c]
1.86	0.606	27.4
	Benzoquinone (2)	
0.018	0.296	56.1
0.048	0.308	53.9
0.080	*0.315*	*52.7*[c]
0.141	0.364	45.6
0.163	0.385	43.1
0.201	0.423	39.3
0.266	0.456	36.4
0.350	0.498	33.3
0.420	0.550	30.2
0.488	0.588	28.3
1.01	*0.599*	*27.7*[c]
1.42	0.606	27.4
2.11	0.606	27.4
	Pyrocatechol (3)	
0.046	0.289	57.4
0.090	0.291	57.0
0.120	*0.296*	*56.1*[c]
0.142	0.320	52.0
0.167	0.381	43.6
0.202	0.430	38.6
0.222	0.456	36.4
0.266	0.482	34.5
0.306	0.503	33.0
0.347	0.541	30.7
0.422	0.564	29.4
0.461	0.581	28.6
0.628	*0.590*	*28.2*[c]
1.26	0.590	28.2
	Methylhydroquinone (4)	
0.046	0.242	68.6
0.110	*0.249*	*66.7*[c]
0.128	0.273	60.9
0.142	0.334	49.8
0.155	0.369	45.0
0.176	0.385	43.1
0.231	0.432	38.4
0.281	0.461	36.1
0.331	0.472	35.2
0.635	0.484	34.3
1.48	*0.494*	*33.6*[c]
1.80	0.498	33.3
	4-Methylpyrocatechol (5)	
0.037	0.230	72.1
0.076	0.240	69.3
0.102	0.247	67.3
0.110	*0.259*	*64.2*[c]
0.132	0.313	53.1
0.145	0.329	50.5
0.181	0.378	43.9
0.241	0.404	41.1
0.286	0.418	39.7
0.375	0.435	38.2
0.417	0.454	36.6
0.551	0.470	35.3
0.625	0.482	34.5
0.864	0.498	33.3
1.00	0.501	33.2
1.06	0.501	33.2
	4-Methylpyrocatechol (5)	
1.25	*0.503*	*33.0*[c]
2.27	0.508	32.7
	tert-Butylhydroquinone (6)	
0.032	*0.221*	*75.2*[c]
0.096	0.247	67.3
0.126	0.263	63.1
0.141	0.287	57.9
0.157	0.303	54.8
0.176	0.338	49.1
0.186	0.350	47.4
0.239	0.371	44.7
0.294	0.390	42.6
0.385	0.395	42.0
0.677	*0.397*	*41.8*[c]
0.930	0.399	41.6
2.06	0.409	40.6
	4-*tert*-Butylpyrocatechol (7)	
0.042	0.216	76.8
0.065	*0.226*	*73.6*[c]
0.090	0.230	72.1
0.127	0.259	64.2
0.167	0.294	56.5
0.205	0.329	50.5
0.250	0.355	46.8
0.342	0.381	43.6
0.450	0.404	41.1
0.508	*0.414*	*40.1*[c]
0.968	0.428	38.8
1.98	0.442	37.6
	2,3-Dimethylhydroquinone (8)	
0.029	0.252	66.0
0.047	*0.252*	*66.0*[c]
0.064	0.273	60.9
0.075	0.299	55.6
0.098	0.322	51.6
0.128	0.338	49.1
0.150	0.348	47.7
0.162	0.357	46.5
0.194	0.381	43.6
0.230	0.411	40.4
0.300	0.447	37.2
0.390	0.463	35.9
0.541	0.487	34.1
1.17	*0.498*	*33.3*[c]
1.70	0.503	33.0
	2,5-Dimethylhydroquinone (9)	
0.021	0.214	77.6
0.079	*0.223*	*74.4*[c]
0.118	0.230	72.1
0.114	0.247	67.3
0.202	0.263	63.1
0.312	0.287	57.9
0.348	0.324	51.2
0.420	0.343	48.4
0.474	0.381	43.6
0.500	0.390	42.6
0.557	0.409	40.6
0.666	0.425	39.0
0.705	*0.437*	*38.0*[c]
0.905	0.442	37.6
1.10	0.447	37.2
1.31	0.468	35.5
1.50	*0.494*	*33.6*[c]
1.63	0.494	33.6
1.80	0.501	33.2
	Durohydroquinone (10)	
0.041	0.200	83.1
0.102	*0.207*	*80.3*[c]
0.306	0.207	80.3
	Tetrafluorohydroquinone (11)	
0.044	0.129	128.5
0.106	0.148	112.1
	Tetrafluorohydroquinone (11)	
0.682	0.200	83.1
1.08	0.268	62.0
1.33	0.320	52.0
1.93	0.371	44.7
2.08	0.432	38.4
2.71	0.477	34.8
3.03	0.606	27.4
3.20	0.637	26.1
4.20	*0.651*	*25.5*[c]
5.38	0.651	25.5
	Hexahydroxybenzene (12)	
0.027	0.221	75.2
0.064	*0.235*	*70.7*[c]
0.110	0.235	70.7
0.120	0.294	56.5
0.133	0.324	51.2
0.200	0.400	41.6
0.220	0.404	41.1
0.327	0.430	38.6
0.440	0.456	36.4
0.672	0.465	35.7
1.09	0.487	34.1
1.32	*0.491*	*33.8*[c]
1.73	0.491	33.8
	2,3-Dihydroxypyridine (13; pH 0)	
0.057	*0.425*	*39.0*[c]
0.118	0.435	38.2
0.157	0.484	34.3
0.196	0.515	32.3
0.223	0.534	31.1
0.251	0.559	29.7
0.332	0.606	27.4
0.410	0.632	26.3
0.450	0.642	25.9
0.711	0.658	25.2
0.976	*0.667*	*24.9*[c]
1.90	0.672	24.7
	2,3-Dihydroxypyridine (13; pH 7)	
0.081	0.606	27.4
0.175	*0.616*	*27.0*[c]
0.326	0.639	26.0
0.509	0.667	24.9
0.796	0.693	24.0
1.20	*0.705*	*23.6*[c]
2.58	0.714	23.2
	3,6-Dihydroxypyridazine (14; pH 7)	
0.082	0.658	25.2
0.158	0.667	24.9
0.500	*0.672*	*24.7*[c]
2.50	0.679	24.5
	Allylhydroquinone (15)	
0.033	0.381	43.6
0.086	*0.397*	*41.8*[c]
0.122	0.400	41.6
0.162	0.423	39.3
0.188	0.442	37.6
0.234	0.456	36.4
0.271	0.475	35.0
0.312	0.484	34.3
0.389	0.494	33.6
0.456	*0.503*	*33.0*[c]
0.515	0.524	31.7
0.574	0.552	30.1
0.600	0.569	29.2
0.772	0.606	27.4
1.05	*0.620*	*26.8*[c]
1.83	0.625	26.6
	4-Allylpyrocatechol (16)	
0.064	0.381	43.6
0.101	*0.385*	*43.1*[c]
0.130	0.430	38.6
0.170	0.456	36.4

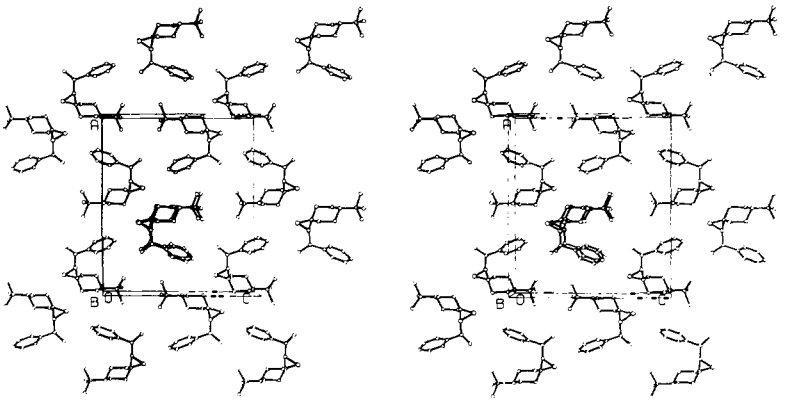

Figure 2. Stereoscopic view of the molecular packing (molecules 3).

Table I. Fractional Atomic Coordinates ($\times 10^4$), Their Estimated Standard Deviations (in Parentheses), and the Equivalent Isotropic Temperature Factors ($Å^2$) for Oxaziridine 3

	x	y	z	B_{eq}
O(1)	4032 (4)	−1271 (12)	2380 (3)	5.99
N(2)	3624 (4)	−2319 (13)	3146 (4)	4.72
C(3)	4230 (6)	−740 (18)	3245 (5)	4.94
C(4)	4942 (5)	−1829 (16)	3579 (5)	5.22
C(5)	4910 (5)	−1723 (16)	4581 (5)	4.79
C(6)	4863 (5)	682 (15)	4890 (5)	4.39
C(7)	4152 (5)	1728 (16)	4517 (5)	5.07
C(8)	4131 (6)	1644 (15)	3511 (5)	4.72
C(9)	2836 (5)	−1506 (15)	3148 (5)	4.75
C(10)	2555 (5)	−1686 (17)	4063 (6)	4.48
C(11)	2693 (5)	−3573 (15)	4528 (6)	5.06
C(12)	2428 (7)	−3680 (20)	5381 (8)	6.76
C(13)	2029 (7)	−2003 (37)	5733 (8)	10.08
C(14)	1877 (7)	−238 (30)	5264 (11)	9.02
C(15)	2149 (6)	19 (22)	4410 (8)	6.57
C(16)	2392 (6)	−2965 (26)	2524 (6)	8.90
C(17)	4883 (5)	815 (15)	5888 (6)	4.66
C(18)	5640 (6)	−33 (16)	6220 (6)	6.28
C(19)	4845 (7)	3228 (17)	6163 (6)	7.44
C(20)	4244 (5)	−383 (18)	6323 (6)	5.87

Table II. Bond Lengths (Å) and Their Estimated Standard Deviations (in Parentheses) for Oxaziridine 3

O(1)-N(2)	1.535 (8)	C(9)-C(10)	1.513 (12)
O(1)-C(3)	1.428 (10)	C(9)-C(16)	1.537 (12)
N(2)-C(3)	1.456 (11)	C(10)-C(11)	1.386 (12)
N(2)-C(9)	1.483 (10)	C(10)-C(15)	1.380 (14)
C(3)-C(4)	1.521 (12)	C(11)-C(12)	1.410 (14)
C(3)-C(8)	1.529 (13)	C(12)-C(13)	1.362 (17)
C(4)-C(5)	1.562 (11)	C(13)-C(14)	1.333 (18)
C(5)-C(6)	1.553 (12)	C(14)-C(15)	1.423 (16)
C(6)-C(7)	1.529 (11)	C(17)-C(18)	1.531 (12)
C(6)-C(17)	1.556 (11)	C(17)-C(19)	1.541 (12)
C(7)-C(8)	1.567 (10)	C(17)-C(20)	1.511 (12)

Table III. Bond Angles (Deg) and Their Estimated Standard Deviations (in Parentheses) for Oxaziridine 3

N(2)-O(1)-C(3)	58.7 (5)	N(2)-C(9)-C(10)	106.7 (7)
O(1)-N(2)-C(3)	57.0 (5)	N(2)-C(9)-C(16)	106.6 (8)
O(1)-N(2)-C(9)	107.8 (6)	C(10)-C(9)-C(16)	112.5 (8)
C(3)-N(2)-C(9)	118.2 (8)	C(9)-C(10)-C(11)	119.5 (9)
O(1)-C(3)-N(2)	64.3 (6)	C(9)-C(10)-C(15)	119.0 (10)
O(1)-C(3)-C(4)	115.2 (8)	C(11)-C(10)-C(15)	121.4 (10)
N(2)-C(3)-C(4)	111.0 (8)	C(10)-C(11)-C(12)	118.1 (10)
O(1)-C(3)-C(8)	116.4 (8)	C(11)-C(12)-C(13)	121.1 (11)
N(2)-C(3)-C(8)	125.4 (8)	C(12)-C(13)-C(14)	119.8 (13)
C(4)-C(3)-C(8)	115.0 (9)	C(13)-C(14)-C(15)	122.2 (14)
C(3)-C(4)-C(5)	107.0 (7)	C(10)-C(15)-C(14)	117.3 (13)
C(4)-C(5)-C(6)	110.5 (8)	C(6)-C(17)-C(18)	109.8 (7)
C(5)-C(6)-C(7)	109.0 (7)	C(6)-C(17)-C(19)	109.0 (8)
C(5)-C(6)-C(17)	110.9 (7)	C(18)-C(17)-C(19)	105.7 (8)
C(7)-C(6)-C(17)	112.0 (7)	C(6)-C(17)-C(20)	113.9 (8)
C(6)-C(7)-C(8)	112.6 (7)	C(18)-C(17)-C(20)	110.1 (8)
C(3)-C(8)-C(7)	107.4 (8)	C(19)-C(17)-C(20)	108.0 (9)

Table IV. Torsion Angles (Deg) for Oxaziridine 3 ($\langle\sigma\rangle < 2°$)

C(3)-O(1)-N(2)-C(9)	113
N(2)-O(1)-C(3)-C(4)	102
N(2)-O(1)-C(3)-C(8)	−119
O(1)-N(2)-C(3)-C(4)	−109
O(1)-N(2)-C(3)-C(8)	105
C(9)-N(2)-C(3)-O(1)	−94
C(9)-N(2)-C(3)-C(4)	158
C(9)-N(2)-C(3)-C(8)	12
O(1)-N(2)-C(9)-C(10)	−155
O(1)-N(2)-C(9)-C(16)	84
C(3)-N(2)-C(9)-C(10)	−94
C(3)-N(2)-C(9)-C(16)	146
O(1)-C(3)-C(4)-C(5)	−161
N(2)-C(3)-C(4)-C(5)	−90
C(8)-C(3)-C(4)-C(5)	60
O(1)-C(3)-C(8)-C(7)	164
N(2)-C(3)-C(8)-C(7)	88
C(4)-C(3)-C(8)-C(7)	−57
C(3)-C(4)-C(5)-C(6)	−59
C(4)-C(5)-C(6)-C(7)	60
C(4)-C(5)-C(6)-C(17)	−176
C(5)-C(6)-C(7)-C(8)	−58
C(17)-C(6)-C(7)-C(8)	179
C(5)-C(6)-C(17)-C(18)	64
C(5)-C(6)-C(17)-C(19)	180
C(5)-C(6)-C(17)-C(20)	−60
C(7)-C(6)-C(17)-C(18)	−174
C(7)-C(6)-C(17)-C(19)	−59
C(7)-C(6)-C(17)-C(20)	62
C(6)-C(7)-C(8)-C(3)	55
N(2)-C(9)-C(10)-C(11)	−45
N(2)-C(9)-C(10)-C(15)	136
C(16)-C(9)-C(10)-C(11)	72
C(16)-C(9)-C(10)-C(15)	−107
C(9)-C(10)-C(11)-C(12)	180
C(15)-C(10)-C(11)-C(12)	−2
C(9)-C(10)-C(15)-C(14)	178
C(11)-C(10)-C(15)-C(14)	0
C(10)-C(11)-C(12)-C(13)	2

The structure of oxaziridine **3** characterized by the *tert*-butyl group and the nitrogen atom, respectively, in equatorial and axial positions on the cyclohexane ring agrees with the conclusions concerning the formation of spirooxaziridines previously suggested by ^1H NMR studies (on the basis of the NMR results, we concluded that the peroxy acid attack occurs from the proequatorial face in imines showing no steric hindrance)[18,19] (Scheme III).

Table I gives the atomic positional parameters, and Tables II to IV show the bond lengths, bond angles, and torsion angles, respectively (see, Experimental Section). Figure 2 describes a stereoview of the molecular packing. The conformation of the molecule can be defined by the angles between the mean plane

(18) Oliveros, E.; Rivière, M.; Lattes, A. *Org. Magn. Reson.* **1976**, *8*, 601-606.

(19) Oliveros, E.; Rivière, M.; Lattes, A. *J. Heterocycl. Chem.* **1980**, *17*, 107-112.

Table III. Fraction of Reversibly Electroactive Adsorbed Species as a Function of the Concentration at Which Adsorption Was Carried Out[a]

compd	C, mM	$\Gamma_{rev\ el}$, nmol cm^{-2}	$\Gamma_{rev\ el}/\Gamma_{total}$[b]
2,5-dihydroxythiophenol (19)	0.067	0.518 ± 0.010	0.96
	0.220	0.524	0.96
	1.50	0.550	0.96
2,5-dihydroxy-4-methylbenzyl mercaptan (20)	0.075	0.700 ± 0.005	0.96
	0.210	0.720	0.98
	0.831	0.726	0.98
allylhydroquinone (15)	0.162	<0.005	
	0.600	0.031 ± 0.005	0.054
	0.772	0.042	0.070
	1.05	0.061	0.10
	1.83	0.070	0.12
phenylhydroquinone (21)	0.155	<0.005	
	0.662	0.026 ± 0.005	0.059
	0.832	0.042	0.082
	0.996	0.047	0.086
	1.22	0.061	0.11
	1.43	0.092	0.16
	1.77	0.103	0.17
2,2',5,5'-tetrahydroxybiphenyl (22)	0.067	<0.02	
	0.450	0.094 ± 0.005	0.27
	0.554	0.122	0.34
	0.605	0.164	0.44
	0.747	0.212	0.52
	0.914	0.263	0.55
	1.14	0.294	0.58
	1.45	0.329	0.61
	1.78	0.352	0.63
	2.20	0.376	0.66
	2.43	0.383	0.67
	2.80	0.388	0.68

[a] Experimental procedures were as described in the text. [b] Values of Γ_{total} are tabulated in Table 1.

2 (A, C, and G). This is as expected because the orientations adopted by these species at low concentrations already represent the densest packing possible.[1,2] Compounds **19** and **20** are reversibly electroactive in the adsorbed state (Table III) whereas compound **14** is not. This can be understood if attachment of **19** and **20** is solely through the sulfur-containing substituent with ring pendant, while **14** is attached to the surface through the ring nitrogen (eq 6).

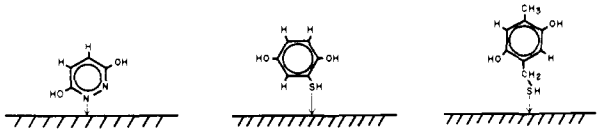

(6)

Durohydroquinone, **10**, and the disulfonated anthraquinones, **25** and **26**, show no tendency toward reorientation even from orientations which are area inefficient (flat).[1] Previous studies[2] showed that the anthraquinones are not reoriented by coadsorption of iodine atoms either. This resistance to reorientation is probably due to an entropy effect: in the flat orientation, the three fused rings can each interact with the Pt surface, whereas the edgewise orientations would permit only limited interaction. Steric hindrance by the sulfonate groups is not responsible for this effect since in compound **25** the 2,3- (or 6,7-) positions are unhindered for η^2 binding. Moreover, as discussed below, sulfonation of 1,2-naphthoquinone, **24**, does not prevent its reorientation. Adsorbed durohydroquinone reorients to a 2,3-η^2 state in the presence of adsorbed iodine.[2] Concentration-dependent reorientation of durohydroquinone is an open question at present due to limited solubility, about 3×10^{-4} M. One cannot rule out the possibility that reorientation may occur at higher concentrations. In fact, another hindered compound, 2,5-dimethylhydroquinone, **9**, reorients to a 2,3-η^2 state, but it does so at concentrations much higher than the corresponding unhindered isomer, 2,3-dimethylhydroquinone, **8** [see below and Figure 2 (E and K)].

Fluorination of the aromatic ring considerably lowers its affinity toward the Pt surface.[7] Accordingly, adsorption of tetrafluorohydroquinone **11** occurs mainly through the phenolic oxygen.[1,2] A close-packed layer is not formed by **11** at low concentrations because interaction between the phenolic oxygen and the Pt surface is comparatively weak. Below about 1.5 mM, Γ increases only slowly with concentration; at higher concentrations, the coverage increases very sharply to the limiting value for the O-η^1 orientation, Figure 2L.

2. Adsorbed Compounds Which Undergo a Single Orientational Transition. The rest of the compounds studied undergo irreversible transitions in which the molecular areas decrease as the concentration is increased above about 1.3×10^{-4} M. The decrease in σ indicates transitions from flat to vertical orientations. Compounds **1–8**, **12**, **13**, **17**, **18**, and **24** each undergo one orientational transition to a state for which σ_p is indicative of edgewise final orientation. There is one exception: at pH 7, compound **13** appears to adopt the endwise N-η^1 orientation. For example, hydroquinone, **1**, undergoes an irreversible transition (eq 7) from the η^6 to the 2,3-η^2 orientation (σ_p = 27.9; calculated σ = 28.6).

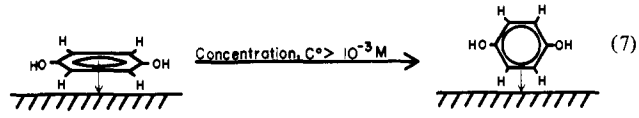

(7)

The same orientational change occurs as a result of exposure of the flat-oriented form to aqueous iodide solution at pH 7.[2] Benzoquinone, **2**, behaves in a manner identical with that of hydroquinone [σ_p = 27.7; calculated σ(2,3) = 27.9]. Pyrocatechol, **3**, irreversibly reorients to either the 2,3- or the 3,4-η^2 orientation (σ_p = 28.2; calculated σ = 26.9); these are indistinguishable on the basis of σ values, although the latter is less hindered. These orientations were found for pyrocatechol in the presence of iodide at pH 7.[2]

Hexahydroxybenzene, **12**, for which only one unique η^2 orientation is possible, reorients abruptly but packs somewhat less densely (σ_p = 33.8) than expected (σ = 28.6). Since the reorientation proceeds readily, this indicates that the OH group by itself does not offer appreciable steric hindrance. By contrast, reorientations of tetramethyl- and 2,5-dimethylhydroquinone requires higher concentrations, presumably due to the influence of the methyl groups (see below). The maximum coverage of methylhydroquinone, **4**, σ_p = 33.6, corresponds to 2,3- or 5,6-η^2 orientation (calculated σ = 33.6); steric hindrance by the methyl group is possible in the 2,3 structure, however. 4-Methylpyrocatechol, **5**, adopts 1,6- and/or 3,4-η^2 orientation (σ_p = 33.0; calculated σ = 31.6); both are sterically hindered, the latter by a methyl group.

When the methyl group in **5** is replaced by an aminoethyl group, as in dopamine, **18**, a significant change is observed in the Γ vs. C curve, Figure 2I: the orientational transition is less abrupt and the upper plateau is reached at considerably higher concentrations. This is most probably the result of protonation of the amine group (in molar acid) which leads to electrostatic repulsion between neighboring molecules of the adsorbed layer. σ_p is 34.8 which most closely corresponds to the unhindered 5,6-η^2 orientation with the protonated amine directed away from the surface (calculated σ = 36.4). Dopamine is still largely protonated at pH 7; accordingly, the shape of the dopamine isotherm resembles that in molar acid. However, the total coverage Γ in neutral medium is everywhere about 0.06 mol cm^{-2} higher than in 1 M acidic solutions. Since a larger proportion of the amine groups are present as the free base at pH 7, the increase in Γ with increasing pH is probably due to additional adsorption through the free amine

(7) Stickney, J. L.; Soriaga, M. P.; Hubbard, A. T.; Anderson, S. E. *J. Electroanal. Chem.* **1981**, *125*, 73.

function. Further evidence for amine attachment is the emergence of a reversibly electroactive species, presumably the N-η^1 attached form,[1] under these conditions.

The molecular areas of *tert*-butylhydroquinone, **6** (σ_p = 41.8), and 4-*tert*-butylpyrocatechol, **7** (σ_p = 40.1) are smaller than might be expected in view of the bulkiness of the *tert*-butyl group. These compounds somehow achieve very efficient packing. The only orientations calculated to fall in this density range are those in which the *tert*-butyl groups are positioned away from the surface. Furthermore, since the thickness of the *tert*-butyl group is more than twice that of the phenyl ring, σ values calculated assuming a uniform thickness equal to that of the *tert*-butyl group are much too large (52–71). Evidently **6** and **7** form an interlocking, η^2 structure such as (viewed from above the surface) shown in eq 8 for which the calculated σ are 43.7 and 42.9, compared with

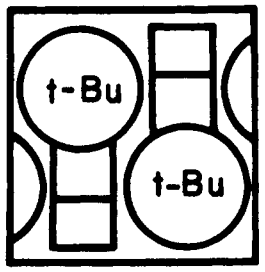

(8)

41.8 and 40.1 found. These reorientations of **6** and **7** resulting from increased concentration resemble those induced by coadsorption of iodide[2] (eq 9).

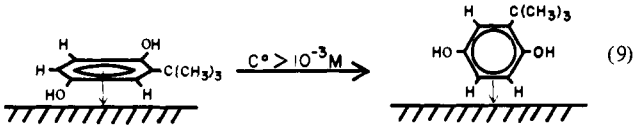

(9)

2,3-Dimethylhydroquinone, **8**, which has substituents in four adjacent positions on the aromatic ring, begins a packing density transition at comparatively low concentrations (5×10^{-5} M) which proceeds to completion less abruptly than is usual. This suggests that placement of the four substituents along one side of the ring decreases the stability of the flat orientation, prompting formation of tilted edgewise ("shingle") structures.[1] The final orientation, σ_p = 33.3, is reached at concentrations above 10^{-3} M when neighboring interactions evidently enforce a fully vertical 5,6-η^2 orientation (calculated σ = 33.6).

The two-ring compound, 1,2-naphthoquinone-4-sulfonic acid, **24**, reorients to an edgewise orientation (σ_p = 45.6), in contrast to the three-ring sulfonated anthraquinones (**25** and **26**) which do not reorient. Either the 1,2- or the 5,6-η^2 structure would account for the result, although the latter which is less hindered might be expected to show reversible electroactivity since the *o*-quinone moiety is not directly bound to the surface. Like the *tert*-butyl group, the sulfonate group has a van der Waals diameter (6.4 Å) greater than the thickness of the phenyl ring. Calculation of molecular area, assuming uniform molecular thickness, that of the sulfonate group, gives a calculated σ for 5,6-η^2 of 60.8, which is much larger than that found (45.0). Evidently an interlocking molecular arrangement is formed (calculated σ = 46.6), as for the *tert*-butyl derivatives (**8**).

Compound **17** contains a long-chain surface-active substituent (hexene). Competition between the phenyl ring and the alkene chain for adsorption on the Pt surface evidently occurs at low concentrations where the measured coverage can only be understood in terms of a mixed layer of η^6-phenyl and alkene-attached species. However, above 2.5×10^{-4} M, reorientation occurs to form only the 5,6-η^2-adsorbed state with the chain extended away from the surface (σ_p = 35.3; calculated σ = 33.6).

The adsorption of 2,3-dihydroxypyridine, **13**, a weak base, is pH dependent. At pH 7 two plateaus are observed. The plateau at concentrations below 2×10^{-4} M is probably due to the 1,6-η^2 orientation ($\sigma_p \approx$ 27.0; calculated σ = 26.9) for which the ring nitrogen and one carbon are adjacent to the surface; above 10^{-3} M, the N-η^1 orientation (eq 10) predominates (σ_p = 23.6; calculated σ = 23.3). The N-η^1 orientation was postulated previously

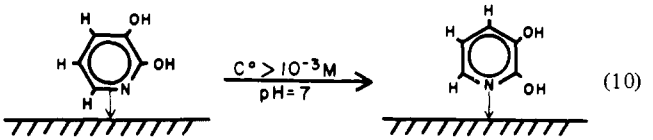

(10)

for compounds of this type on Pt.[8] In molar acid two plateaus are again observed, but the low-concentration layer corresponds to a mixture of η^6 and edgewise or endwise orientations. Although the experiment does not identify the endwise or edgewise orientations, the most likely possibilities are those in which the ring nitrogen remains protonated in the adsorbed state. Above 10^{-3} M, the η^6 form reorients (σ_p = 24.9), leaving what is probably a mixture of η^2 orientations.

3. Adsorbed Compounds Which Undergo Multiple Orientational Transitions. Six of the compounds studied (**9**, **15**, **16**, **21–23**) display two or more irreversible transitions as concentration is increased. For example, the adsorption isotherm of 2,5-dimethylhydroquinone, **9**, shows three distinct plateaus, Figure 2E. The low-concentration plateau corresponds to the η^6 orientation.[1] The intermediate plateau (3×10^{-4} to 1×10^{-3} M) corresponds to the 3,4-η^2 orientation (σ_p = 38.0; calculated σ = 39.2). Above 10^{-3} M, a final reorientation (eq 11) occurs, yielding the more hindered but also more area-efficient 2,3-η^2 state (σ_p = 33.6; calculated σ = 33.6). When exposed to aqueous iodide, η^6-adsorbed 2,5-dimethylhydroquinone reoriented to a mixture of 3,4- and 2,3-η^2 species.[2] These irreversible transitions occur at higher concentration than for 2,3-dimethylhydroquinone, **9**, presumably due to steric hindrance. The influence of steric hindrance is demonstrated by tetramethylhydroquinone (**10**), which shows no tendency to reorient up to its solubility, 3×10^{-4} M although it reorients as a result of coadsorption of iodine.[2]

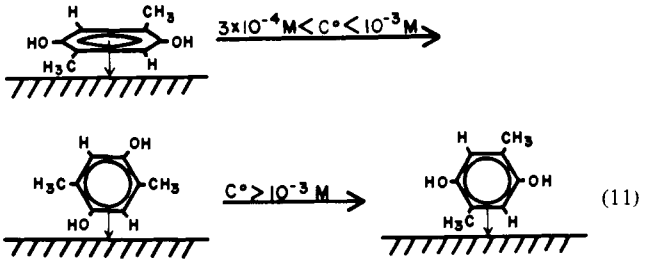

(11)

The two orientational transitions of 1,4-dihydroxynaphthalene, **23**, are unexpected in view of the fact that the sulfonated analogue **24** displays only one transition and that **23** itself is displaced but not rereoriented by aqueous iodide in molar acid.[2] Molecular area calculations show that no single edgewise or endwise orientation can account for the second plateau (σ_p = 39.5); tilted or mixed orientations are the remaining possibilities. In fact, if the fused phenyl ring is considered as a 3,4 substituent on the hydroquinone framework, the structure of **23** resembles that of 2,3-dimethylhydroquinone, **8**, for which bulky groups are situated along one side of the aromatic ring and for which a tilted η^2 orientation was very readily formed.[1] By analogy, the intermediate plateau for **23** most likely corresponds to a tilted 2,3-η^2 orientation. Likewise, the third or highest coverage plateau occurs when, at the limiting density, neighboring interactions enforce a fully vertical 2,3 edgewise orientation (σ_p = 29.7; calculated σ = 28.6). This structure implies that the hydroquinone ring is adsorbed preferentially over the phenyl ring and is supported by the studies on phenylhydroquinone, **21**, and 2,2′,5,5′-tetrahydroxybiphenyl, **22** (see below).

Allylhydroquinone, **15**, and allylpyrocatechol, **16**, have surface-active substituents which may lead to differing modes of attachment. The low-concentration plateau for allylhydroquinone (σ_p = 41.8) corresponds to a mixture of η^6-phenyl- and allyl-at-

(8) Gland, J. L.; Somorjai, G. A. *Adv. Colloid Interface Sci.* **1976**, *5*, 205.

tached species; the same is true for allylpyrocatechol (σ_p = 43.1). Between 10^{-4} and 5×10^{-4} M, the adsorbed molecules reorient exclusively to edgewise orientations. The unhindered 5,6-η^2-allylhydroquinone (σ_p = 33.0; calculated σ = 33.6) and the 1,6-η^2-4-allylpyrocatechol (σ_p = 32.4; calculated σ = 31.6) are the most likely possibilities. These same η^2 orientations were observed in the presence of coadsorbed iodine.[2] At concentrations above 5×10^{-4} M, a second transition occurs. This is probably due to formation of a mixed layer consisting of edgewise phenyl- and allyl-attached species. This is supported by the data in Table III which show that, at the maximum coverage of allylhydroquinone, about 12% of the adsorbed molecules are reversibly electroactive. If *all* of the allyl-attached molecules (σ = 14)[9] are reversibly electroactive, then the remaining species must be present in the 1,2-η^2 orientation (σ = 29.6). It is important to note that allyl attachment alone does not give rise to reversible electroactivity since essentially none was observed at the low-concentration plateau even though allyl-attached species are thought to be present; presumably certain orientations of neighboring adsorbed molecules promote reversibly electroactive behavior of the allyl-attached molecules. Other factors such as the flexibility of the alkene side chain may also be important.[10]

The low-concentration plateau of phenylhydroquinone, **21** (σ_p = 83.1), corresponds to a parallel orientation in which both aromatic rings are adsorbed flat on the Pt surface (σ = 85.1);[1] the same holds for 2,2′,5,5′-tetrahydroxybiphenyl, **22** (σ_p = 84.1; calculated σ = 85.1). Above 10^{-4} M phenylhydroquinone undergoes reorientation to a η^4 structure in which both aromatic rings are edgewise to the surface (σ_p = 43.1; calculated σ = 39.8). This same flat-to-edgewise reorientation occurred under the influence of aqueous iodide. Similarly, 2,2′,5,5′-tetrahydroxybiphenyl reorients from the flat to the edgewise orientation, most probably as shown in eq 12 (σ_p = 47.1; calculated σ = 39.8). Apparently

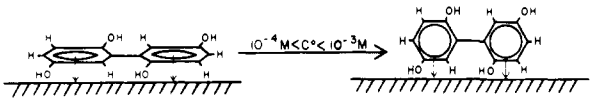

(12)

the phenyl rings are not perfectly coplanar, since σ_p is higher than the calculated σ. As the concentration is increased above 10^{-3} M, a third plateau is reached [σ_p(**21**) = 28.2; σ_p(**22**) = 29.0], for which the σ_p values correspond most closely to η^2 orientations in which only one of the aromatic rings is directly bonded to the Pt surface. The 3,4-η^2 orientation (eq 13) of compound **22** gives best agreement (calculated σ = 28.6). This structure is also borne

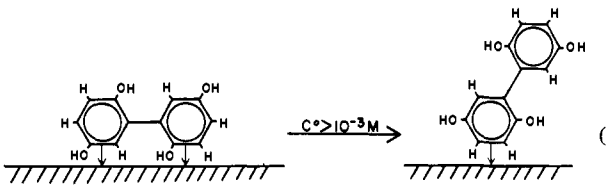

(13)

out by the data in Table III which show that, at the highest-coverage plateau, 68% of the adsorbed tetrahydroxybiphenyl is reversibly electroactive. The electroactivity occurs presumably because, in the 3,4-η^2 structure, one hydroquinone ring is not directly bound to the Pt surface. However, the fact that not all of the adsorbed material displays reversible electroactivity suggests that there are multiple requirements for electrochemical reactivity of adsorbed molecules, not all of which are met for all molecules in this instance. In contrast, only about 17% of the η^2-adsorbed phenylhydroquinone is reversibly electroactive. This implies that η^2 attachment of phenylhydroquinone occurs primarily through the hydroquinone moiety, causing inactivation of that electroactive center. That is, the highest coverage plateau for phenylhydroquinone (eq 14) is due to η^2 states of which the 5,6-η^2 orientation

(9) Lane, R. F.; Hubbard, A. T. *J. Phys. Chem.* **1973**, *77*, 1411.
(10) Lane, R. F.; Hubbard, A. T. *J. Phys. Chem.* **1973**, *77*, 1401.

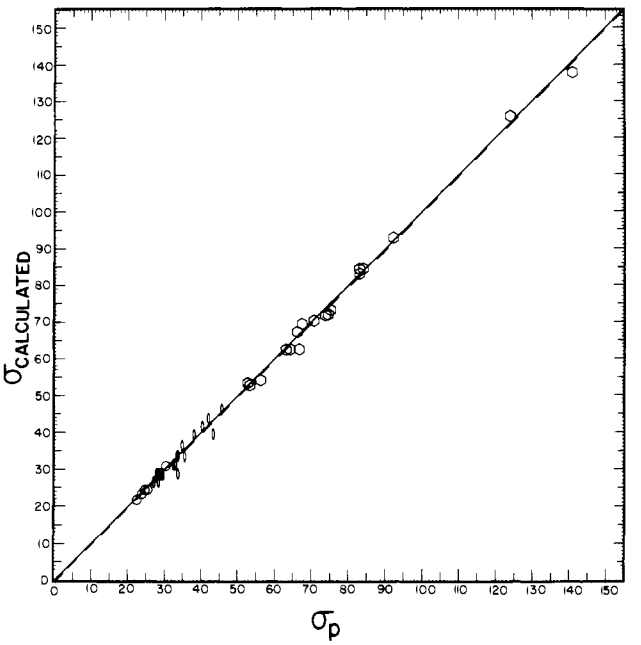

Figure 4. Experimental coverage at the plateaus in Figure 2, expressed as area (Å^2) per adsorbed molecule, σ_p, graphed against calculated σ for the molecular orientations assigned in the text: hexagon, flat orientation; ellipse, η^2 (edgewise) orientation; circle, η^1 (endwise) orientation. Ten σ_p values postulated to correspond to tilted or mixed orientations are not included among the 45 points shown in the figure. Numerical values are listed in Table I. Solid line represents ideal correlation between measured σ_p and calculated σ. Dashed line represents linear least-squares lines for which the slope equals 0.999, the intercept equals −0.404, and the correlation coefficient equals 0.997.

predominates (calculated σ = 28.6). A similar η^2 orientation was found for 1,4-dihydroxynaphthalene, **23**.

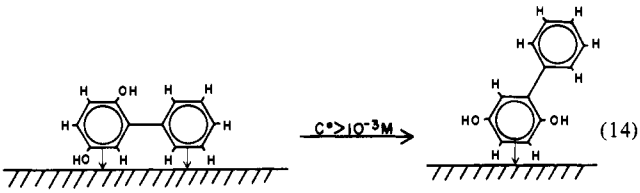

(14)

4. Goodness-of-Fit of the Orientation Assignments. The reliability of the molecular orientation assignments can be assessed from a graph of σ values calculated for the assigned orientations against measured values, σ_p (Figure 4). Values calculated for each flat orientation are denoted by hexagons, while those for edgewise and endwise structures are denoted by ellipses and circles, respectively. Of the 55 σ_p values, ten are thought to correspond to tilted or mixed orientations; since a tilting angle or a combination of two or more orientations can always be found which yields perfect agreement with σ_p, these ten values were not included in Figure 4. As the figure shows, theory agrees with experiment over the full range, which includes a sevenfold variation in molecular area. Linear regression analysis of σ calculated vs. σ gives the following: slope = 0.999; intercept = −0.404; correlation coefficient = 0.997.

Conclusions

Packing density, orientation, and mode of attachment of molecules adsorbed on smooth platinum electrodes in solution are dependent on the solute concentration. Under the present conditions, namely, 2.5×10^{-6} M to 5×10^{-3} M aromatic in 1 M aqueous perchlorate: (i) aromatic molecules are irreversibly adsorbed on platinum; (ii) the orientational transitions which occur as the solute concentration is increased are likewise irreversible; (iii) mono- and bicyclic homoaromatic molecules adsorb flat at low concentrations but reorient to edgewise orientations at higher concentrations; (iv) the most stable η^2 orientations are those which occupy minimal surface area and for which the ring edge closest

the electrode does not contain bulky substituents; (v) anthraquinones are adsorbed parallel to the surface and are not influenced by changes in concentration; (vi) the biphenyl moiety, initially adsorbed with both rings parallel to the surface, undergoes reorientation first to a structure in which both rings are bonded to the surface edgewise and then to a η^2 structure in which one ring is attached and the other is pendant; (vii) preferential adsorption of organic functional groups on Pt follows the order thiol > N heteroaromatic > diphenol ring ≈ quinonoid ring > benzene ring > alkene > amine > hydroxyl > ketone; (viii) in general, adsorbed molecules reorient to structures occupying smaller surface area.

Acknowledgment is made to the donors of the Petroleum Research Fund, administered by the American Chemical Society, and to the Air Force Office of Scientific Research for support of this research. Dr. D. L. Fields, Eastman Kodak Co., Rochester, NY, provided a pure sample of compound **20**. Professor Clifford S. Benton, Westmont College, Santa Barbara, CA, prepared compound **22**.

Registry No. 1, 123-31-9; **2**, 106-51-4; **3**, 120-80-9; **4**, 95-71-6; **5**, 452-86-8; **6**, 1948-33-0; **7**, 98-29-3; **8**, 608-43-5; **9**, 615-90-7; **10**, 527-18-4; **11**, 771-63-1; **12**, 608-80-0; **13**, 16867-04-2; **14**, 123-33-1; **15**, 5721-21-1; **16**, 1126-61-0; **17**, 81255-51-8; **18**, 51-61-6; **19**, 2889-61-4; **20**, 81753-11-9; **21**, 1079-21-6; **22**, 4371-32-8; **23**, 571-60-8; **24**, 2066-93-5; **25**, 117-14-6; **26**, 84-50-4; Pt, 7440-06-4.

A Nitrogen-15 Nuclear Magnetic Resonance Study of the Acid–Base and Tautomeric Equilibria of 4-Substituted Imidazoles and Its Relevance to the Catalytic Mechanism of α-Lytic Protease[1]

John D. Roberts,* Chun Yu,[2] Cynthia Flanagan, and Theresa R. Birdseye

Contribution No. 6537 from the Laboratories of Chemistry, California Institute of Technology, Pasadena, California 91125. Received September 23, 1981

Abstract: The pH dependence of the ^{15}N NMR shifts of histamine, imidazole-4-propionic acid, imidazole-4-acetic acid, *trans*- and *cis*-urocanic acid, and *endo-cis*-3-(4-imidazoyl)bicyclo[2.2.1]hept-5-ene-2-carboxylic acid has been determined at the natural-abundance level of ^{15}N. The chemical-shift changes permit calculation of pK_a values for the acidic species present as well as reasonably accurate positions of the N1(H) ⇌ N3(H) tautomeric equilibria for those species having unprotonated imidazole rings. The ^{15}N shifts of *cis*-urocanic acid and *endo-cis*-3-(4-imidazoyl)bicyclo[2.2.1]hept-5-ene-2-carboxylic acid demonstrate that carboxylate–N3(H) hydrogen-bonding interactions can cause the N3(H) tautomers to be substantially more stable than the N1(H) tautomers. The unusual positions of these tautomeric equilibria are quite similar to that found for the histidine of the catalytic triad of α-lytic protease.

Imidazole rings are very important functional groups in many biological processes. In connection with the present research, the role of the histidine imidazole ring in the Asp-His-Ser catalytic triad of the serine protease is especially relevant.[3] For histidine, as with all 4-substituted imidazoles, the position of the N1(H)–N3(H) tautomeric equilibrium (eq 1) is potentially significant. In water solution, this equilibrium is established rapidly

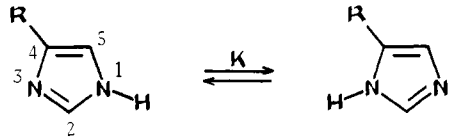

(1)

on the NMR time scale, and even with ^{15}N NMR wherein the nitrogen resonances of the azine and N–H are expected to have chemical-shift differences of about 83 ppm,[4] the resonances are quite sharp[5] as expected for a mean lifetime before tautomeric proton shift of less than 10^{-4} s.

The equilibrium shown in eq 1 as a function of pH for histidine has been very carefully studied by Blomberg, Maurer, and Rüterjans[6] with the aid of ^{15}N NMR spectroscopy. The shift changes of the imidazole nitrogens of histidine are shown in Figure 1. Four levels of protonation (1–4) are covered in the pH range that was studied and, of these, it is evident from the shifts that a significant change in the equilibrium shown in eq 1 occurs in the change from **3** to **4**. The first ionization of histidine (**1** ⇌ **2**) has pK_a 1.8,[7] and on the change from **1** to **2** there appears to be no significant change in the ^{15}N shifts.[6] The second ionization (**2** ⇌ **3**) has pK_a 6.0[7] and deprotonation of the imidazole ring leads to a 53-ppm ^{15}N chemical-shift difference between N1 and N3

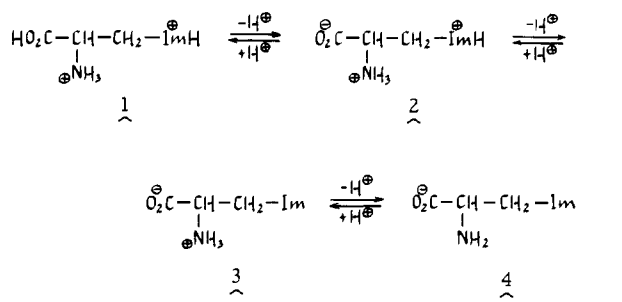

(1) Supported by the National Science Foundation and the National Institutes of Health.

(2) On leave from the Institute of Photographic Chemistry of the Academia Sinica, Peking, 1979–1981.

(3) Bachovchin, W. W.; Roberts, J. D. *J. Am. Chem. Soc.* **1978**, *100*, 8041–8047.

(4) (a) Schuster, I. I.; Roberts, J. D. *J. Org. Chem.* **1979**, *44*, 3864–3867. (b) See also: Alei, M., Jr.; Morgan, L. O.; Wageman, W. E.; Whaley, T. W. *J. Am. Chem. Soc.* **1980**, *102*, 2881–2887.

(5) Paramagnetic metals may cause serious line broadening of histidine resonances quite independently of proton-exchange processes.[3]

(6) Blomberg, R.; Maurer, W.; Rüterjans, H. *J. Am. Chem. Soc.* **1977**, *99*, 8149–8159.

(7) Perrin, D. D. "Dissociation of Organic Bases in Solution"; Butterworths: New York, 1965; p 385.

0002-7863/82/1504-3945$01.25/0